

Modulating Singlet Fission through Interchromophoric Rotation

Sohan D. Jadhav, Devika Sasikumar and Mahesh Hariharan*

School of Chemistry, Indian Institute of Science Education and Research Thiruvananthapuram
(IISER- TVM), Maruthamala P.O., Vithura, Thiruvananthapuram 695551, Kerala, India

Electronic Supplementary Information (ESI)

Contents

Section A : Methods and Materials.....	S2
○ Computational methods.....	S2
○ Estimation of energy of the charge transfer state.....	S2
○ Transition charge method using the transition charge from electrostatic potential (TrESP).....	S3
Section B : Tables.....	S3
○ Table S1. Effective excitonic coupling, effective energies, ΔE_{SF} and effective SF coupling at all rotational offsets for long-axis displacement $x = 0.6 \text{ \AA}$	S3
○ Table S2. Effective excitonic coupling, effective energies, ΔE_{SF} and effective SF coupling at all rotational offsets for long-axis displacement $x = 1.6 \text{ \AA}$	S4
Section C : Figures.....	S5
○ Figure S1. (a) TD-DFT calculated S_1 state in terrylene that corresponds entirely to the transition between the HOMO and LUMO frontier molecular orbitals. (b) TD-DFT calculated natural transition orbitals of the T_1 state.....	S5
○ Figure S2. Terrylene dimer model with interplanar distance fixed for the calculations.....	S5
○ Figure S3. Transfer integrals or Fock (one-electron coupling) matrix elements (in meV).....	S6

- **Figure S4.** 2D mapping of the charge transfer state energy E_{CT} (in meV) as a function of rotation angle and long axis displacement.....S6
- **Figure S5.** Absolute values of transfer integrals or Fock (one-electron coupling) matrix elements (in meV).....S7

Section D: References.....S7

Section A : Materials and Methods

Computational methods

All calculations were carried out with the CAM-B3LYP functional¹ and the 6-31G* basis set using Gaussian 16.² CAM-B3LYP was preferred over B3LYP considering the improved performance of the long-range correction in handling excited states especially with a large charge transfer (CT) component.³ The terrylene monomer was geometry optimised and placed at specific long axis displacements and rotations using Avogadro 1.2.0.^{4,5}

The charge transfer integrals (coupling matrix elements) were calculated using the CATNIP tool version 1.9⁶ using the output of energy calculations of the monomers and dimers from Gaussian 16.² The wavefunctions should be orthogonal for accurate magnitudes of charge transfer coupling.⁷ Natural transition orbitals (NTOs) were generated using Multiwfn 3.7.⁸ Calculations of all quantities and subsequent generation of the 2D mappings were carried out utilizing the NumPy and Matplotlib libraries on Python.

Estimation of energy of the charge transfer state

The energy of the charge transfer state were estimated using the equation^{9,10}

$$E_{CT} = IP - EA + V_{coul} \quad (\text{eq S1})$$

Ionisation potential (IP) and electron affinity (EA) were evaluated from the single point energies of the geometry-optimised neutral monomer, cation and anion of terrylene.

$$IP = E_{cation} - E_{neutral}$$

$$EA = E_{neutral} - E_{anion}$$

V_{coul} is the Coulomb interaction between the Mülliken atomic charges of the anion and cation evaluated using the expression,

$$V_{coul} = \frac{1}{4\pi\epsilon_0} \sum_i \sum_j \frac{q_i q_j}{|r_i - r_j|} \quad (\text{eq S2})$$

where q_i (q_j) is the Mülliken charge on atom i (atom j) of monomer 1 (monomer 2) in a dimer. Likewise, r_i (r_j) represents the position vectors of atom i (atom j) of monomer 1 (monomer 2) in a dimer. The Mülliken charges were obtained from the respective Gaussian output files.

Transition charge method using the transition charge from electrostatic potential (TrESP)

For closely packed chromophoric frameworks, accurate values of the Coulombic coupling J_{coul} can be obtained through the transition charge method using TrESP.¹¹ J_{coul} was evaluated for the $S_1 \leftarrow S_0$ transition by replacing the Mülliken charges with transition charges in eq S2. The calculation was implemented in the Multiwfn 3.7 program package.⁸

Section B : Tables

Table S1. Effective excitonic coupling, effective energies, ΔE_{SF} and effective SF coupling at all rotational offsets for long-axis displacement $x = 0.6 \text{ \AA}$. All values are in meV.

θ	ΔE_{FE}	ΔE_{TT}	$ J_{eff} $	E'_{FE}	$E'_{FE} - J_{eff} $	E'_{TT}	ΔE_{SF}	$ V'_{SF} $
0°	1253.90	465.27	1381.64	1036.10	-345.53	1734.73	2080.27	766.54
5°	1075.74	424.53	1212.12	1214.26	2.14	1775.47	1773.34	677.78
10°	658.66	321.54	809.66	1631.34	821.68	1878.46	1056.77	461.04
15°	257.76	194.82	411.70	2032.24	1620.54	2005.18	-384.64	224.75
20°	45.14	80.83	192.56	2244.86	2052.30	2119.17	-66.87	60.97
25°	0.04	11.24	140.62	2289.96	2149.34	2188.76	-39.42	0.36
30°	14.53	6.12	139.66	2275.47	2135.81	2193.88	-58.07	8.42
35°	28.84	62.28	125.66	2261.16	2135.50	2137.72	-2.22	31.23
40°	34.26	163.80	119.86	2255.74	2135.88	2036.20	99.68	39.64
45°	34.87	299.38	107.36	2255.13	2147.77	1900.62	247.15	51.25
50°	43.60	450.70	126.63	2246.40	2119.77	1749.30	370.48	97.45
55°	78.92	577.20	164.04	2211.08	2047.04	1622.80	424.24	182.52

60°	140.44	631.75	210.86	2149.56	1938.70	1568.25	370.45	272.51
65°	201.72	590.66	249.48	2088.28	1838.80	1609.34	229.46	322.10
70°	227.41	467.82	153.31	2062.59	1909.27	1732.18	177.09	305.11
75°	202.53	304.64	228.63	2087.47	1858.84	1895.36	-36.52	229.22
80°	140.27	149.27	165.67	2149.73	1984.07	2050.73	-66.67	127.31
85°	77.59	40.53	85.54	2212.41	2126.87	2159.47	-32.60	42.58
90°	51.50	1.76	0.00	2238.50	2238.50	2198.24	40.26	9.86

Table S2. Effective excitonic coupling, effective energies, ΔE_{SF} and effective SF coupling at all rotational offsets for long-axis displacement $x = 1.6 \text{ \AA}$. All values are in meV.

θ	ΔE_{FE}	ΔE_{TT}	$ J_{eff} $	E'_{FE}	$E'_{FE} - J_{eff} $	E'_{TT}	ΔE_{SF}	$ V'_{SF} $
0°	425.52	331.99	270.13	1864.48	1594.35	1868.01	-273.67	44.20
5°	376.50	310.67	228.59	1913.50	1684.91	1889.33	-204.42	16.73
10°	264.22	251.94	121.43	2025.78	1904.35	1948.06	-43.71	35.34
15°	152.25	167.21	2.81	2137.75	2134.94	2032.79	102.15	59.19
20°	71.99	76.84	85.73	2218.01	2132.28	2123.16	9.12	37.73
25°	22.42	14.39	146.69	2267.58	2120.89	2185.61	-64.72	2.87
30°	8.77	7.57	120.77	2281.23	2160.46	2192.43	-31.97	1.47
35°	32.12	59.43	144.97	2257.88	2112.91	2140.57	-27.66	40.77
40°	71.15	166.64	35.70	2218.85	2183.15	2033.36	149.79	110.70
45°	97.02	328.54	194.02	2192.98	1998.96	1871.46	127.50	170.79
50°	98.29	513.63	183.33	2191.71	2008.38	1686.37	322.01	191.31
55°	80.27	652.78	151.94	2209.73	2057.78	1547.22	510.57	167.63
60°	55.48	686.24	114.23	2234.52	2120.29	1513.76	606.53	119.02
65°	32.73	604.39	80.28	2257.27	2177.00	1595.61	581.39	67.90
70°	16.02	447.10	35.62	2273.98	2238.36	1752.90	485.47	29.21
75°	6.00	271.88	35.98	2284.00	2248.02	1928.12	319.90	7.53
80°	1.47	125.47	22.58	2288.53	2265.96	2074.53	191.43	0.31
85°	0.17	32.55	11.13	2289.83	2278.70	2167.45	111.25	0.80
90°	0.02	1.18	0.00	2289.98	2289.98	2198.82	91.16	0.15

Section C : Figures

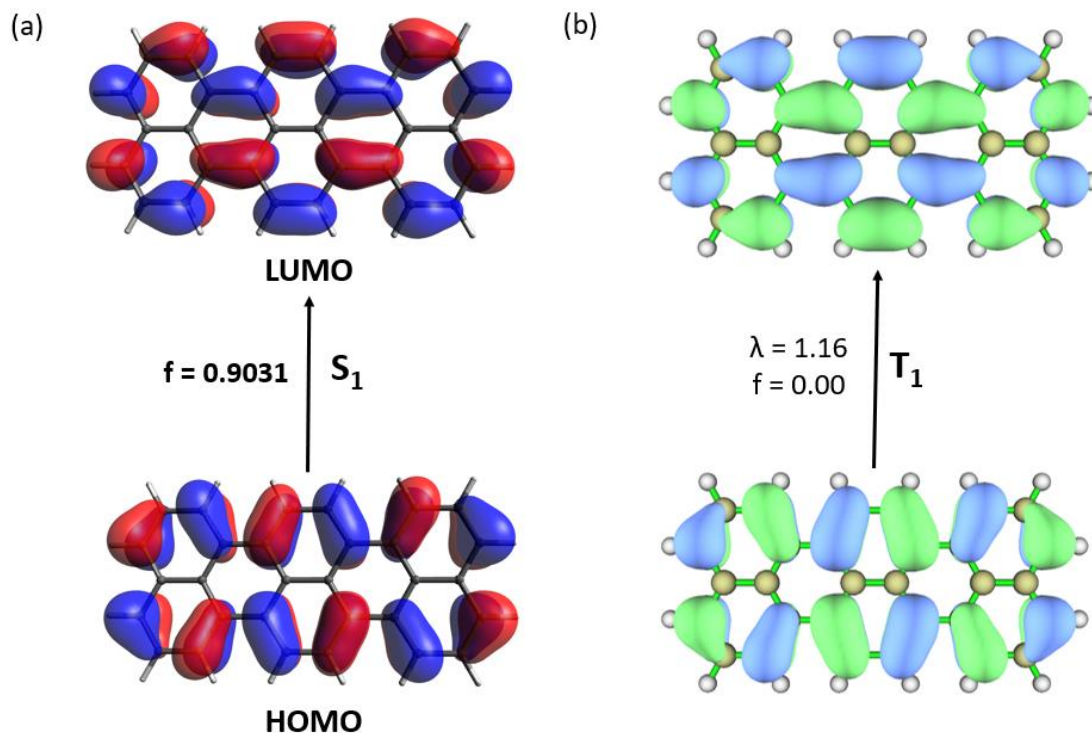


Figure S1. (a) TD-DFT calculated S_1 state in terrylene that corresponds entirely to the transition between the HOMO and LUMO frontier molecular orbitals (FMOs). (b) TD-DFT calculated NTOs i.e., orbitals involved in hole-particle excitation of the T_1 state (involves contribution from multiple orbitals) where λ is the weightage of the NTO and f is the oscillator strength. (isovalue = 0.02)

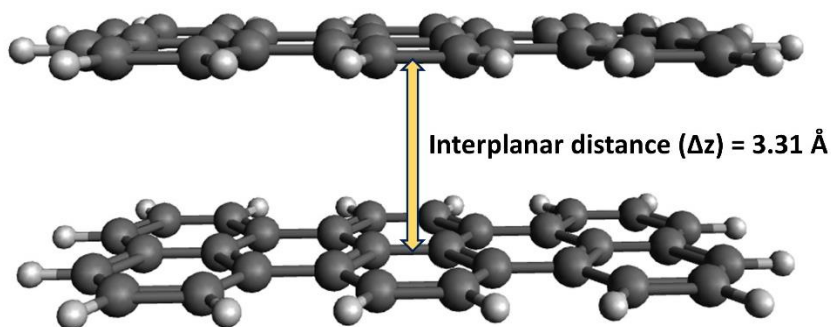


Figure S2. Terrylene dimer model with interplanar distance fixed for the calculations.

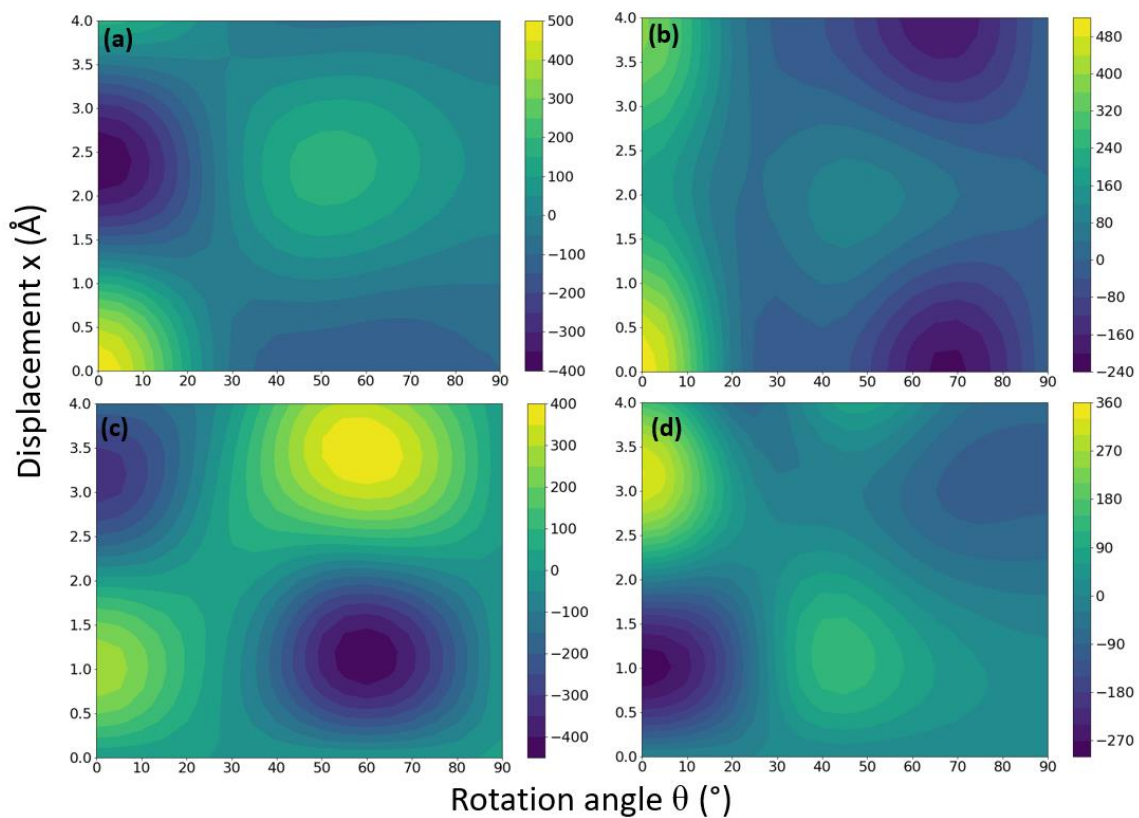


Figure S3. Transfer integrals or Fock (one-electron coupling) matrix elements (in meV).

(a) F_{HH} (b) F_{LL} (c) F_{HL} (d) F_{LH}

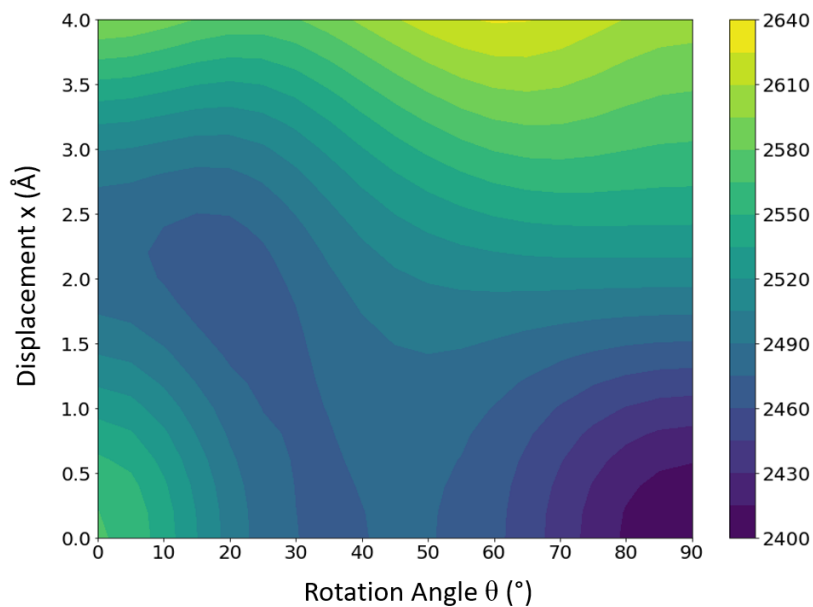


Figure S4. 2D mapping of the charge transfer state energy E_{CT} (in meV) as a function of rotation angle and long axis displacement.

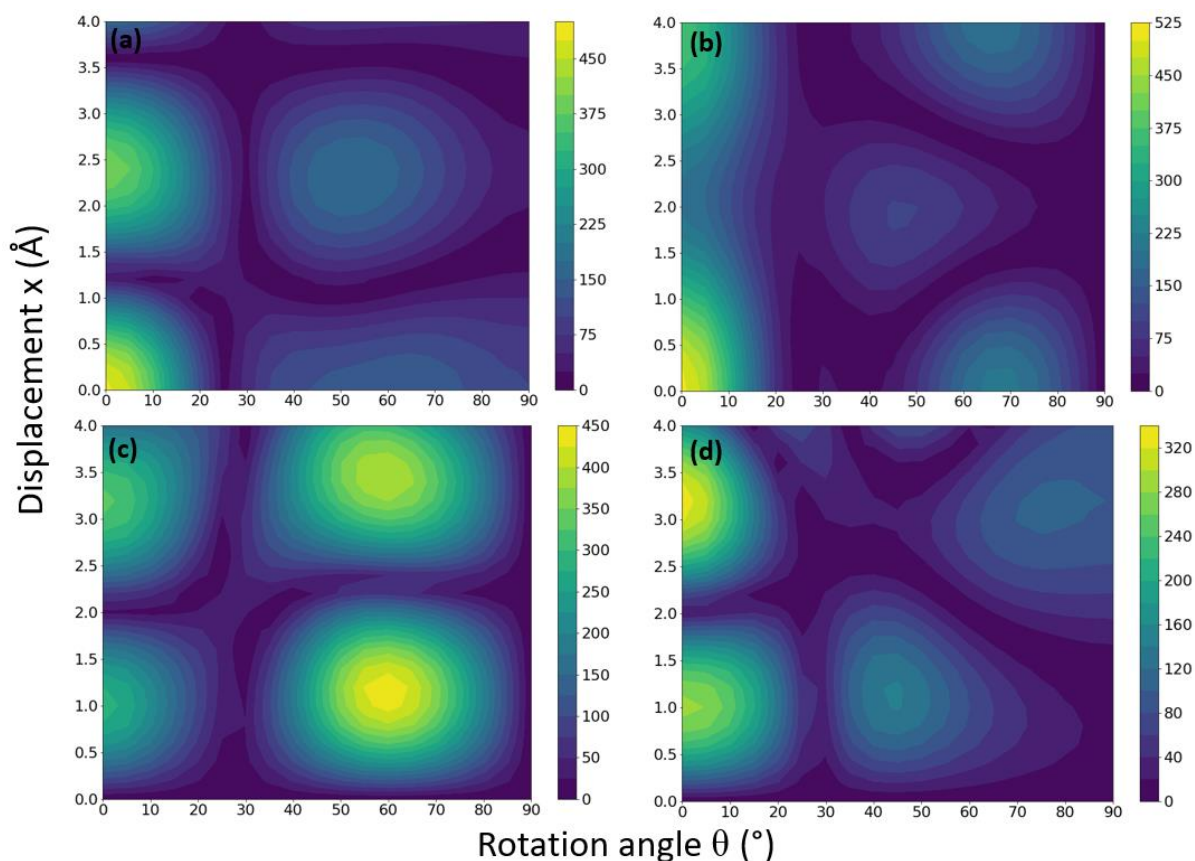


Figure S5. Absolute values of transfer integrals or Fock (one-electron coupling) matrix elements (in meV). (a) $|F_{HH}|$ (b) $|F_{LL}|$ (c) $|F_{HL}|$ (d) $|F_{LH}|$

Section D: References

- 1 T. Yanai, D. P. Tew and N. C. Handy, A new hybrid exchange–correlation functional using the Coulomb-attenuating method (CAM-B3LYP), *Chem. Phys. Lett.*, 2004, **393**, 51–57.
- 2 M. J. Frisch, G. W. Trucks, H. B. Schlegel, G. E. Scuseria, M. A. Robb, J. R. Cheeseman, G. Scalmani, V. Barone, G. A. Petersson, H. Nakatsuji, X. Li, M. Caricato, A. V. Marenich, J. Bloino, B. G. Janesko, R. Gomperts, B. Mennucci, H. P. Hratchian, J. V. Ortiz, A. F. Izmaylov, J. L. Sonnenberg, D. Williams-Young, F. Ding, F. Lipparini, F. Egidi, J. Goings, B. Peng, A. Petrone, T. Henderson, D. Ranasinghe, V. G. Zakrzewski, J. Gao, N. Rega, G. Zheng, W. Liang, M. Hada, M. Ehara, K. Toyota, R. Fukuda, J. Hasegawa, M. Ishida, T. Nakajima, Y. Honda, O. Kitao, H. Nakai, T. Vreven, K. Throssell, J. A. Montgomery, Jr., J. E. Peralta, F. Ogliaro, M. J. Bearpark, J. J. Heyd, E.

- N. Brothers, K. N. Kudin, V. N. Staroverov, T. A. Keith, R. Kobayashi, J. Normand, K. Raghavachari, A. P. Rendell, J. C. Burant, S. S. Iyengar, J. Tomasi, M. Cossi, J. M. Millam, M. Klene, C. Adamo, R. Cammi, J. W. Ochterski, R. L. Martin, K. Morokuma, O. Farkas, J. B. Foresman, and D. J. Fox, Gaussian 16, Revision C.01, Gaussian, Inc., Wallingford CT, 2016
- 3 I. V. Rostov, R. D. Amos, R. Kobayashi, G. Scalmani and M. J. Frisch, Studies of the ground and excited-state surfaces of the retinal chromophore using CAM-B3LYP, *J. Phys. Chem. B*, 2010, **114**, 5547–5555.
 - 4 Avogadro: An Open-Source Molecular Builder and Visualization Tool. Version 1.2.0. [Http://Avogadro.Cc/](http://Avogadro.Cc/).
 - 5 M. D. Hanwell, D. E. Curtis, D. C. Lonie, T. Vandermeersch, E. Zurek and G. R. Hutchison, Avogadro: an advanced semantic chemical editor, visualization, and analysis platform, *J. Cheminform.*, 2012, **4**, 17.
 - 6 GitHub - JoshuaSBrown/QC_Tools: This Small Repository Provides Functionality for Calculating the Charge Transfer Integrals between Two Molecules. [Https://Github.Com/JoshuaSBrown/QC_Tools](https://Github.Com/JoshuaSBrown/QC_Tools).
 - 7 E. F. Valeev, V. Coropceanu, D. A. da Silva Filho, S. Salman and J.-L. Brédas, Effect of Electronic Polarization on Charge-Transport Parameters in Molecular Organic Semiconductors, *J. Am. Chem. Soc.*, 2006, **128**, 9882–9886.
 - 8 T. Lu and F. Chen, Multiwfn: A multifunctional wavefunction analyzer, *J. Comput. Chem.*, 2012, **33**, 580–592.
 - 9 D. Casanova, Theoretical Modeling of Singlet Fission, *Chem. Rev.*, 2018, **118**, 7164–7207.
 - 10 S. Ito, T. Nagami and M. Nakano, Singlet fission in pancake-bonded systems, *Phys. Chem. Chem. Phys.*, 2017, **19**, 5737–5745.
 - 11 M. E. Madjet, A. Abdurahman and T. Renger, Intermolecular Coulomb Couplings from Ab Initio Electrostatic Potentials: Application to Optical Transitions of Strongly Coupled Pigments in Photosynthetic Antennae and Reaction Centers, *J. Phys. Chem. B*, 2006, **110**, 17268–17281.